

Spatially Constrained Generative Adversarial Networks for Conditional Image Generation

Songyao Jiang¹ · Hongfu Liu² · Yue Wu¹ · Yun Fu^{1,3}

Received: date / Accepted: date

Abstract Image generation has raised tremendous attention in both academic and industrial areas, especially for the conditional and target-oriented image generation, such as criminal portrait and fashion design. Although the current studies have achieved preliminary results along this direction, they always focus on class labels as the condition where spatial contents are randomly generated from latent vectors. Edge details are usually blurred since spatial information is difficult to preserve. In light of this, we propose a novel Spatially Constrained Generative Adversarial Network (SCGAN), which decouples the spatial constraints from the latent vector and makes these constraints feasible as additional controllable signals. To enhance the spatial controllability, a generator network is specially designed to take a semantic segmentation, a latent vector and an attribute-level label as inputs step by step. Besides, a segmentor network is constructed to impose spatial constraints on the generator. Experimentally, we provide both visual and quantitative results on *CelebA* and *DeepFashion* datasets, and demonstrate that the pro-

posed SCGAN is very effective in controlling the spatial contents as well as generating high-quality images.

Keywords Image synthesis · Spatial constraints · Segmentor network · Generative models · Adversarial training

1 Introduction

The success of Generative Adversarial Networks (GAN) (Goodfellow et al., 2014) upsurges an increasing trend of realistic image synthesis (Zhao et al., 2017; Zhang et al., 2017; Wang et al., 2018b), where a generator network produces artificial samples to mimic the real samples from a given dataset and a discriminator network attempts to distinguish between the real samples and artificial samples. These two networks are trained adversarially as two players in a game, which can be modelled and explained using the game theory. Eventually, the two-player game will end up with a solution called the Nash Equilibrium. In such equilibrium, the generator is capable of mapping a latent vector from a simple distribution to real data samples from a complex distribution, while the discriminator can hardly distinguish the artificial samples from the real ones. GANs have been widely used in many applications such as natural language processing (Zhang et al., 2016; Yu et al., 2017), image super-resolution (Ledig et al., 2017; Liu et al., 2017c), domain adaptation (Hoffman et al., 2016; Bousmalis et al., 2017), object detection (Li et al., 2017a), activity recognition (Li et al., 2017b), video prediction (Mathieu et al., 2015), face aging (Liu et al., 2017b), semantic segmentation (Luc et al., 2016), and image-to-image translations (Isola et al., 2017; Zhu et al., 2017a). These methods adopt the adversarial training

Songyao Jiang
E-mail: syjiang@ece.neu.edu

Hongfu Liu
E-mail: hongfuliu@brandeis.edu

Yue Wu
E-mail: yuewu@ece.neu.edu

Yun Fu
E-mail: yunfu@ece.neu.edu

¹ Department of Electrical and Computer Engineering, Northeastern University, Boston, MA, USA.

² Department of Computer Science, Brandeis University, Waltham, MA, USA.

³ College of Computer and Information Science, Northeastern University, Boston, MA, USA.

to their tasks in order to obtain more accurate results and improve the performance.

However, GAN focuses on learning a marginal distribution and generates random artificial data samples, which neglects joint distribution or conditional distribution. Beyond generating arbitrary images, conditional and target-oriented image generation is highly needed for various practical scenarios, such as criminal portraits based on descriptions from victims, clothing design with certain fashion elements, data augmentation and artificial intelligence imagination. Mirza and Osindero (2014) first provided a way of conditional generation according to input class labels, which is further extended by Odena et al. (2017) and Chongxuan et al. (2017) that additional classifiers are utilized to guide the image generation. Although the current studies have achieved preliminary results along this direction, they always focus on available class labels as the condition where spatial contents are still randomly constructed from latent vectors. The mapping between latent vectors and spatial contents remains as a black box that there is barely a way to explicitly specify the spatial components of the synthesized images. In other words, images generated by GAN based methods are not spatially controllable. As a side effect, the edge details are usually blurred and the boundary information is difficult to preserve due to the lack of spatial constraints. For example, Pix2Pix (Isola et al., 2017) is good at style transfer. But when training on face datasets, it struggles to preserve the spatial information and sometimes generates the “ghost faces”. Odena et al. (2017) guide the image generation with the auxiliary class labels or attributes. These semantic attributes cannot reflect the spatial information, which leads to low-quality images.

As mentioned above, the spatial information is crucial to provide high-quality features for synthesized images and increase the model controllability for target-oriented image generation. In light of this, we focus on the image generation with additional spatial constraints besides class-label condition. The spatial constraints can be provided by semantic segmentations. Our target is to utilize the rich spatial information within the semantic segmentations as constraints and guide the generator to synthesize artificial images that comply with those spatial constraints. Our task is different from the image-to-image translation task as follows. Our goal is to simulate a joint distribution of images with their spatial and class-level conditions, and provide diverse results generated from a combination of input semantic segmentations, class labels and randomly sampled latent vectors. But image-to-image translation enforces

an one-to-one mapping between domains, which cannot provide diverse results from a single input.

Generally speaking, we propose a novel Spatially Constrained Generative Adversarial Network (SCGAN), which decouples the spatial constraints from the latent vector and makes these constraints available as additional control signal inputs. SCGAN consists of three networks, a generator network, a discriminator network with an auxiliary classifier and a segmentor network, which are trained together adversarially. The generator is specially designed to take a semantic segmentation, a latent vector and an attribute label as inputs step by step to synthesize a fake image following their joint distribution. The discriminator network tries to distinguish between real images and generated images as well as classifying them into attributes. The discrimination and classification results guide the generator to synthesize realistic images with correct target attributes. The segmentor network attempts to conduct semantic segmentations on both real images and fake images to deliver estimated segmentations, which guides the generator in synthesizing spatially constrained images. With those networks, the proposed SCGAN generates realistic images guided by semantic segmentations and attribute labels, which enables many interesting applications such as interpolating faces from their left faces to their right faces, and generating intermediate faces from not smiling to smiling facial expression.

In this paper, we elaborate each component of our proposed SCGAN in detail, and introduce the objective functions with training algorithms to optimize it. Experimentally, we demonstrate the effectiveness and benefits of the spatial constraints by providing both qualitative and quantitative results on two datasets including a face dataset called *CelebA* (Liu et al., 2015) and a fashion dataset called *DeepFashion* (Liu et al., 2016). We show plenty of high-quality results generated from the proposed SCGAN including some interesting features such as generating faces with continuously varying expressions and orientation. We also show our failure cases with an improper generator configuration, and discuss a particular design to avoid them. An analysis of the training strategy and an ablation study on the model convergence are also provided. Here we highlight our major contributions as follows.

- A novel Spatially Constrained Generative Adversarial Network (SCGAN) is proposed with both spatial and attribute-level controllability, where a segmentor network is designed to guide the generator network with spatial information preserved, and increase the model stability for convergence.
- To avoid foreground-background mismatch, we particularly design the generator network to extract

spatial information from input segmentation first, then concatenate a latent vector to provide variations, and finally use attribute labels to synthesize attribute-specific contents in the generated image.

- Extensive experiments on the *CelebA* and *DeepFashion* datasets demonstrate the superiority of proposed SCGAN over representative GAN based methods and image-to-image translation methods in visual quality and controllability.

The remainder of the paper is structured as follows. In Section 2, an overview of the literature on generative models, 3D morphable models and image-to-image translation methods is given. Section 3 provides some preliminary knowledge on GAN based models. Section 4 presents the methodology of our proposed SCGAN. Experimental results are shown and discussed in Section 5. Finally, Section 6 summarizes this paper, draws a conclusion and suggests ideas for future work.

2 Related Work

In recent years, deep generative models inspired by GAN (Goodfellow et al., 2014) enable computers to imagine new samples based on the knowledge learned from the given datasets. There are many variations of GAN to improve the generating ability. DCGAN (Radford et al., 2015) provides a general network architecture for image synthesis. InfoGAN (Chen et al., 2016) learns an interpretable representation in latent vectors. BEGAN (Berthelot et al., 2017) leverages an autoencoder-like discriminator to eliminate artifacts. WGAN (Arjovsky et al., 2017) introduces Wasserstein distance to solve the training difficulties and mode-collapse problem of GAN, which improves the visual quality and variation of generation. WGAN is further improved by adding a gradient penalty term in optimizing the discriminator (Gulrajani et al., 2017). CoupleGAN (Liu and Tuzel, 2016) couples two GANs with shared weights to generate paired image samples. A new normalization method called spectrum normalization is introduced by Miyato et al. (2018) to further stabilize the GAN training. AmbientGAN (Bora et al., 2018) tries to solve the lossy measurement problem by adding a measurement function to the GAN framework. Most recently, PG-GAN (Karras et al., 2018) utilizes a progressive growing training strategy to generate high-resolution images which achieves state-of-the-art visual quality.

In the meanwhile, many researchers focused on developing some target-oriented generative models instead of random generation. Conditional GAN (cGAN) (Mirza and Osindero, 2014) is the first attempt to input conditional labels into both generator and discriminator

to achieve conditional image generation. Similarly, AC-GAN (Odena et al., 2017) constructs an auxiliary classifier within the discriminator to output classification results and TripleGAN (Chongxuan et al., 2017) introduces a classifier network as an extra player to the original two players setting. CasualGAN (Kocaoglu et al., 2018) tends to make cGAN more creative by allowing sampling from an interventional distribution. However, all these studies focus on attribute-level conditions and neglect spatial conditions, which leads to the lack of spatial controllability in synthesized images.

When it comes to spatial controllability, we refer to the ability of manipulating the spatial contents of the generated images. People have been working on such topics using a 3D approach since 1990s. Vetter (1998) proposed a way of synthesizing novel views from a single face image. A more powerful manipulation can be achieved by using 3D morphable models (Blaiz and Vetter, 1999; Matthews et al., 2007; Genova et al., 2018; Egger et al., 2018). Those methods reconstruct 3D morphable models from input 2D images, where the contents can then be manipulated, such as changing the face shape, face orientation, facial attribute, and facial expression. The morphed 3D model can also be rendered back to 2D images afterwards. Compared with GAN based generative models, one limitation of morphable models is that they cannot effectively render realistic and diverse contents beyond their 3D models, such as background, clothes, or body parts.

For GAN based image-to-image translation methods, the input images can be regarded as spatial conditions in image translation. An image-to-image translation networks called Pix2Pix is proposed by Isola et al. (2017), which uses an image as the conditional input and trains their networks with supervision from paired images. Their method can generate realistic street view images based on their semantic segmentations. Many researchers find out that paired training is unnecessary after introducing a cycle-consistency loss. Inspired by this finding, they propose several unpaired image-to-image translation methods (Zhu et al., 2017a; Kim et al., 2017; Yi et al., 2017; Liu et al., 2017a). Based on those two-domain translation methods, StarGAN (Choi et al., 2018) proposes a multi-domain image translation network by utilizing an auxiliary classifier. Most recently, Wang et al. (2018a) further extended the Pix2Pix to a video-to-video synthesis framework called Vid2Vid, which translates an input video sequence to an output video sequence in the target domain. Vid2Vid enables many interesting applications such as synthesizing dance videos from skeleton videos. However, all the above approaches have an intrinsic assumption of one-

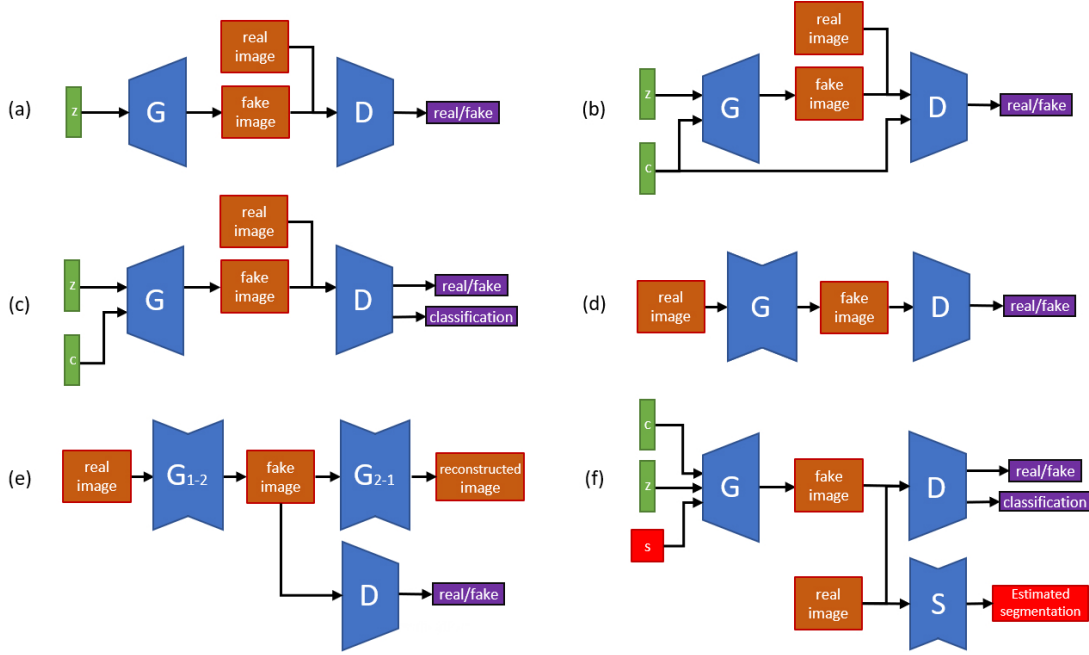


Fig. 1 Illustrations of the difference between our proposed SCGAN and some other well-known GAN models: (a) Vanilla GAN (Goodfellow et al., 2014); (b) cGAN (Mirza and Osindero, 2014); (c) ACGAN (Odena et al., 2017); (d) Pix2Pix (Isola et al., 2017); (e) CycleGAN (Zhu et al., 2017a); (f) Our proposed SCGAN.

to-one mapping without any variation between two domains, which may not hold for one-to-many tasks.

Different from all existing methods, our proposed SCGAN takes latent vectors, attribute labels and semantic segmentations as inputs, and decouples the image generation into a three-dimension synthesis task. By this means, SCGAN is capable of controlling the spatial contents, attributes and generating target images with a large diversity.

3 Preliminary Knowledge

We provide preliminary knowledge on generative adversarial networks and their extended methods related to our proposed method. We briefly summarize and compare their approaches in terms of model and losses. This knowledge could help in understanding our methodology, seeing the our difference, and recognizing the novelty of our proposed SCGAN.

Goodfellow et al. (2014) proposed the novel GAN framework to estimate a generative model using an adversarial training strategy. The framework can be depicted in Figure 1(a). The discriminator D and the generator G act as two adversarial players in a min-max game with an optimization criterion

$$\mathbb{E}_{x \sim p_{data}} [\log D(x)] + \mathbb{E}_{z \sim p_z} [\log (1 - D(G(z)))], \quad (1)$$

where x is a real data sample from a real target data distribution \mathbb{P}_{data} , z is a random latent vector sampled

from a simple distribution \mathbb{P}_z . G is subject to minimize the above criterion while D tries to maximize it. The final goal is to generate realistic fake data $G(z)$ which cannot be distinguished from x . Goodfellow et al. (2014) provided proofs for the existence of a global minimum and the convergence of the framework. Experiments on MNIST (LeCun et al., 1998), TFD (Susskind et al., 2010) and CIFAR-10 (Krizhevsky and Hinton, 2009) datasets are conducted to show their ability of generating images in the target data distribution. This GAN framework is usually referred as “Vanilla GAN”.

Following the future work described by Goodfellow et al. (2014), Mirza and Osindero (2014) constructed a conditional GAN framework (cGAN) to control the generated results based on conditional class labels. As described in Figure 1(b), in this framework, a conditional class label c is fed into G together with a random latent vector z to generate a fake sample $G(z, c)$. When discriminating the fake sample from the real one, D also takes c as an additional input to ensure that the generated sample follows the joint data distribution $\mathbb{P}(x, c)$ as well. Different from cGAN, Odena et al. (2017) enforced the generated sample $G(z, c)$ to be consistent with c by utilizing an auxiliary classifier D_c embedded in D with a classification loss described as

$$\mathbb{E}_{x,c} [-\log D_c(c|x)] + \mathbb{E}_{z,c} [-\log (D_c(c|G(z, c)))]. \quad (2)$$

Replacing the input conditional class label c in cGAN with an input image x and utilizing a encoder-decoder-

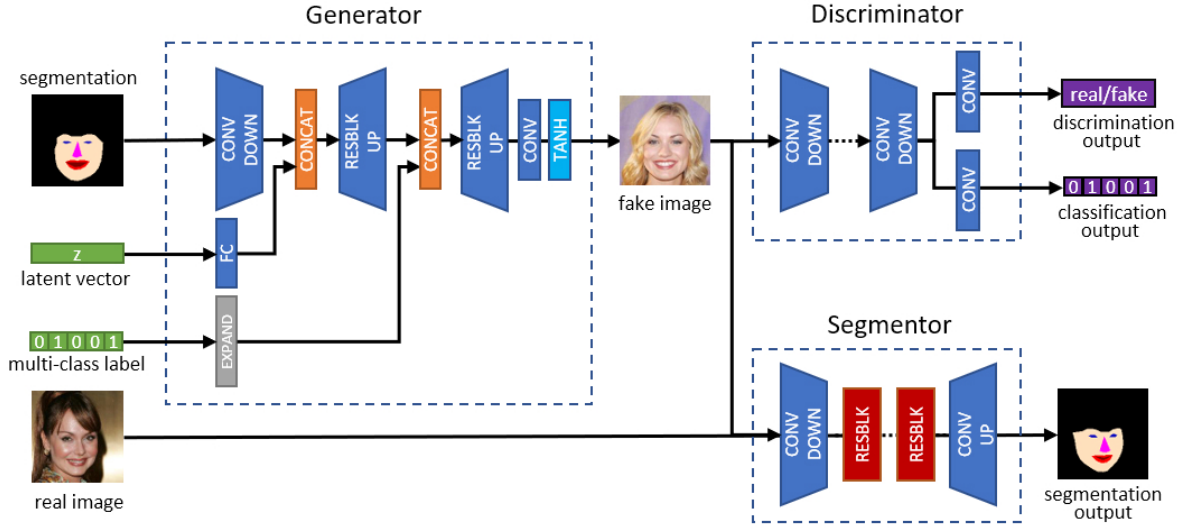


Fig. 2 SCGAN framework. SCGAN consists of a generator, a discriminator with auxiliary classifier and a segmentor which are trained together. The generator is particularly designed that a semantic segmentation, a latent vector and an attribute label are input to the generator step by step to generate a fake image. The discriminator takes either fake or real image as input and output a discrimination result and a classification result. Similar to discriminator, the segmentor takes either fake or real image as input and output a segmentation result which is compared to the ground-truth segmentation to calculate a segmentation loss, which guides the generator to synthesize fake images which comply with the input segmentation.

like G called U-Net, Isola et al. (2017) were the first to propose an GAN based image-to-image translation networks named Pix2Pix, which is trained using paired images, as shown in Figure 1(d). They argued that G always ignores the input z , so they removed it from the framework and learned an one-to-one mappings from one domain to another. In fact, this is due to the supervision from paired images. Our study will show that input latent vectors could still contribute to the generated diversity. Following the paired image translation idea, Zhu et al. (2017a) proposed an GAN based unpaired image translation method called CycleGAN with two generators $G_{1 \rightarrow 2}$ and $G_{2 \rightarrow 1}$ (see Figure 1(e)), which form a cycle of translating x from a source domain to a target domain ($G_{1 \rightarrow 2}(x)$) and then back to the source domain ($G_{2 \rightarrow 1}(G_{1 \rightarrow 2}(x))$). A cycle-consistency loss is adopted to optimize the above cycle, which is expressed as

$$\mathbb{E}_x [\|x - G_{2 \rightarrow 1}(G_{1 \rightarrow 2}(x))\|_1]. \quad (3)$$

During its training process, CycleGAN contains another cycle which translate an real input image from the target domain to the source domain using $G_{2 \rightarrow 1}$, and reconstruct it back to the target domain via $G_{1 \rightarrow 2}$. The objective of introducing the cycle-consistency loss is to keep the basic contents of the input image consistent during the image translation process, which avoids the requirement of paired images for training in Pix2Pix, since paired images are hard to obtain in many cases. Due to this cycle-consistency loss, their approach also

enforces an one-to-one mapping between domains without any diversity in translated images.

A brief illustration of our proposed SCGAN is also provided in Figure 1(f) for comparison. SCGAN utilizes a novel segmentor network to guide the generator for spatially constrained image synthesis. In the next section, we will elaborate the methodology of our proposed SCGAN, and explain how SCGAN acquires the spatial controllability and diversity in its generated results.

4 Methodology

In this section, we first give a definition of our target problem and define the symbols used in our methodology. Then we talk about the framework structure of proposed SCGAN. After that, all loss terms in the objective functions which optimize those networks are discussed in detail. Eventually we provide a training algorithm for the proposed SCGAN.

4.1 Problem Setting

Image generation is to synthesize realistic images which cannot be distinguished from the real images in a given target dataset. Our goal aims to employ spatial constraints to generate high-quality images with target-oriented controllability of their spatial contents. Let $\mathbb{P}(x, c, s)$ denote the joint distribution of the target dataset, where x is a real image of size $(H \times W \times 3)$ with H and W

as the height and width, c is its multi-attribute label of size $(1 \times n_c)$ with n_c as the number of attributes, and s is its semantic segmentation of size $(H \times W \times n_s)$ with n_s as the number of segmentation classes. Each pixel in s is represented by an one-hot vector with dimension n_s , which codes the semantic index of that pixel. Our problem can be defined as $G(z, c, s) \rightarrow y$, where $G(\cdot, \cdot, \cdot)$ is the generating function, z is the latent vector of size $(1 \times n_z)$, c defines the target attributes, s acts as a high-level and pixel-wise spatial constraint, and y is the conditionally generated image which complies with the target conditions c and s . Our target can be expressed as training a deep generator network to fit the target mapping function $G(z, c, s) \rightarrow y$, where the joint distribution $\mathbb{P}(y, c, s)$ is expected to follow the same distribution as $\mathbb{P}(x, c, s)$.

4.2 Spatially Constrained Generative Adversarial Networks

In this paper, we propose a generative model called Spatially Constrained Generative Adversarial Networks (SCGAN) to help training a generator networks to fit the target mapping function $G(z, c, s) \rightarrow y$. Our proposed SCGAN consists of three networks shown in Figure 2, which are a generator network G , a discriminator network D and a segmentor network S . Here we introduce each network individually in detail, define their objective functions, and provide a training algorithm to optimize these networks.

4.2.1 Generator Network

We utilize a generator network G to match our desired mapping function $G(z, c, s) \rightarrow y$. Our generator takes three inputs which are a latent code z , an attribute label c and a target segmentation map s . As shown in Figure 2, these inputs are fed into the generator step by step in orders. First, the generator G takes s as input and extracts spatial information contained in s by several downsampling convolutional layers. After that, the convolution result is concatenated with a dimensional expansion of z in channel dimension. After a few upsampling residual blocks (RESBLKUP in Figure 2), c is fed into the generator at last to guide the generator to generate attribute-specific images that contain basic image contents generated from s and z . Details of the upsampling residual block can be found in Figure 3.

This particular design of G follows the idea of “from the whole to the detail”. In other words, G first decides the spatial configuration of the synthesized image according to the spatial constraints extracted from s . Then G forms the basic structure (e.g., background,

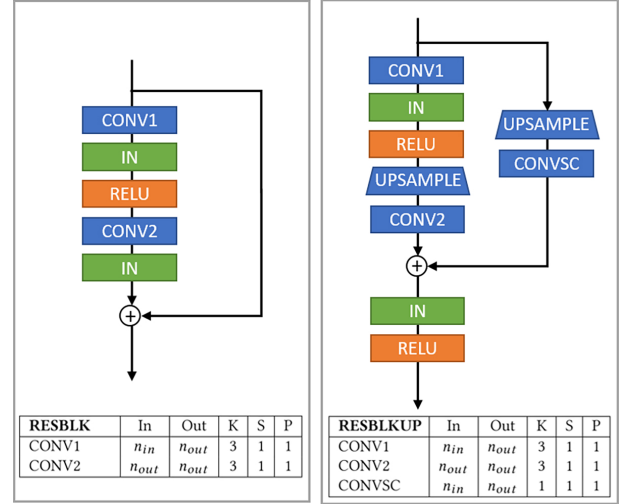


Fig. 3 Structure of the RESBLK and RESBLKUP blocks used in SCGAN. (Abbrev: In=Input channel size; Out=Output channel size; CONV=Convolutional layer; IN=Instance Normalization; RELU=Rectified linear unit; UPSAMPLE=Upsampling using nearest neighbor; K=Kernel size; S=Stride; P=Zero paddings.)

ambient lighting) of the generated image using the information coded in z . After that, G generates the attribute components of the synthesized images specified by c . This particular design has some useful features as follows. When keeping s and z fixed, inputting different attribute labels into G will result into synthesized images with different attributes but sharing the same lighting condition, same background, and same spatial configuration. When keeping s and c fixed and inputting different latent vectors, G will synthesize images with the same spatial configuration and the same attributes but diverse details. Fixing z and c while alternating s will change the spatial configuration but keep the attributes and details unchanged, such as generating the face images of a same person with different expressions and facial orientations. We will show the advantage of this configuration and provide the results of varying every single inputs in the experiment section.

4.2.2 Discriminator Network

To obtain realistic results which can hardly be distinguished from the real images, we employ a discriminator network D which forms a GAN framework with G . An auxiliary classifier is embedded in D to do a multi-class classification which provides attribute-level and domain-specific information back to G . D is defined as $D : x \rightarrow \{D_d(x), D_c(x)\}$, where $D_d(x)$ gives the probability of x belonging to the real data distribution and $D_c(x)$ outputs the probabilities of x belonging to n_c attribute-level domains. D and G act as two

adversarial players during training and will eventually reach the Nash Equilibrium that the joint distribution of the $\mathbb{P}(G(z, c, s), c)$ becomes very close to $\mathbb{P}(x, c)$.

4.2.3 Segmentor Network

We propose a segmentor network S to provide spatial constraints in conditional image generation. Let $S(\cdot)$ be the mapping function. S takes either real or generated image data as input and outputs the probabilities of pixel-wise semantic segmentation results of size $(H \times W \times n_s)$. S can be trained solely using x with its corresponding s . When training the other networks SCGAN, the weights in S can be fixed, and S can still provide the gradient information to G . Training S separately speeds up the model convergence and reduces the memory usage of the GPUs. However, in our experiment, training S together with G and D leads to better visual quality. We will provide and discuss comparison results in Section 5.7.

4.2.4 Overall Objective

The overall objective function of SCGAN to optimize S , D and G can be represented as

$$\mathcal{L}_S = \mathcal{L}_{seg}^{real}, \quad (4)$$

$$\mathcal{L}_D = -\mathcal{L}_{adv} + \lambda_{cls} \mathcal{L}_{cls}^{real}, \quad (5)$$

$$\mathcal{L}_G = \mathcal{L}_{adv} + \lambda_{cls} \mathcal{L}_{cls}^{fake} + \lambda_{seg} \mathcal{L}_{seg}^{fake}, \quad (6)$$

where \mathcal{L}_S , \mathcal{L}_D and \mathcal{L}_G are objective functions to optimize S , D and G . \mathcal{L}_{adv} is adversarial loss, \mathcal{L}_{cls} is classification loss and \mathcal{L}_{seg} is segmentation loss. λ_{seg} and λ_{cls} are hyper-parameters which control the relative importance of \mathcal{L}_{seg} and \mathcal{L}_{cls} compared to \mathcal{L}_{adv} . In the following subsections, each term in these objectives will be introduced one by one.

4.2.5 Adversarial Loss

To generate realistic images which cannot be distinguished from original data. We adopt a conditional objective from Wasserstein GAN with gradient penalty (Gulrajani et al., 2017) which can be defined as

$$\mathcal{L}_{adv} = \mathbb{E}_x [D_a(x)] + \mathbb{E}_{z,c,s} [D_a(G(z, c, s))] + \lambda_{gp} \mathbb{E}_{\hat{x}} [(\|\nabla_{\hat{x}} D_a(\hat{x})\|_2 - 1)^2], \quad (7)$$

where $G(z, c, s)$ is the generated image conditioned on both attribute label c and segmentation s , λ_{gp} controls

the weight of gradient penalty term, \hat{x} is the uniformly interpolated samples between a real image x and its corresponding fake image $G(z, c, s)$. During the training process, D and G act as two adversarial players that D tries to maximize this loss while G tries to minimize it.

4.2.6 Segmentation Loss

We propose a segmentation loss which acts as a spatial constraint to regulate the generator to comply with the spatial information defined by the input semantic segmentation. The proposed real segmentation loss to optimize the segmentor network S can be described as

$$\mathcal{L}_{seg}^{real} = \mathbb{E}_{x,s} [A_s(s, S(x))], \quad (8)$$

where $A_s(\cdot, \cdot)$ computes cross-entropy pixel-wisely by

$$A_s(a, b) = - \sum_{i=1}^H \sum_{j=1}^W \sum_{k=1}^{n_s} a_{i,j,k} \log b_{i,j,k}, \quad (9)$$

where a is the ground-truth segmentation and b is the estimated segmentation of a of size $(H \times W \times n_s)$. Taking a real image x as input, estimated segmentation $S(x)$ is compared with ground-truth segmentation s to optimize the segmentor S . When training together with the generator G , the segmentation loss term to optimize G is defined as

$$\mathcal{L}_{seg}^{fake} = \mathbb{E}_{z,c,s} [A_s(s, S(G(z, c, s)))], \quad (10)$$

where the segmentor takes the fake image generated by the generator $G(z, c, s)$ as input and output a estimated segmentation $S(G(z, c, s))$, which is compared with input segmentation s to the generator. By minimizing this loss term in the full objective \mathcal{L}_G , the generator is forced to generate fake images which are consistent with the input semantic segmentations s .

4.2.7 Classification Loss

We embed an auxiliary multi-attribute classifier D_c which shares the weights with D_d in discriminator D except the output layer. D_c enables the proposed SCGAN to generate attribute conditioned images. Similar to an ordinary multi-attribute classifier, the auxiliary classifier D_c takes an image as input and classify the image into independent probabilities of n_c attribute labels. During training the model, D_c learns to classify input images into their attribute labels by optimizing the classification loss for real samples defined as

$$\mathcal{L}_{cls}^{real} = \mathbb{E}_{x,c} [A_c(c, D_c(x))], \quad (11)$$

Algorithm 1: Spatially Constrained Generative Adversarial Networks. In our experiment, $\lambda_{cls} = 5$, $\lambda_{seg} = 1$, $\lambda_{gp} = 10$, $n_{repeat} = 5$ and the batch size $m = 16$.

```

1 Initialize three network parameters  $\theta_G, \theta_D, \theta_S$ ;
2 while  $\theta_G$  has not converged do
3   for  $n = 1, \dots, n_{repeat}$  do
4     Sample a batch of latent vectors
        $\{z^i\}_{i=1}^m \sim \mathcal{N}(0, 1)$ ;
5     Sample a batch of real images, attribute labels
       and semantic segmentations  $\{x^i, c^i, s^i\}_{i=1}^m$ 
       from data distribution  $\mathbb{P}_{data}(x, c, s)$ ;
6     Sample a batch of numbers  $\{\epsilon^i\}_{i=1}^m \sim \mathcal{U}(0, 1)$ ;
7      $\{s_t^i\}_{i=1}^m \leftarrow \text{shuffle}(\{s^i\}_{i=1}^m)$ ;
8     for  $i = 1, \dots, m$  do
9        $\tilde{x}^i \leftarrow G(z^i, c^i, s_t^i)$ ;
10       $\hat{x}^i \leftarrow \epsilon^i x^i + (1 - \epsilon^i) \tilde{x}^i$ ;
11       $\mathcal{L}_{adv}^i \leftarrow D_d(\tilde{x}^i) - D_d(x^i)$ 
12         $+ \lambda_{gp} (\|\nabla_{\tilde{x}} D_d(\tilde{x}^i)\|_2 - 1)^2$ ;
13       $\mathcal{L}_{cls}^{real, i} \leftarrow A_c(c^i, D_c(x^i))$ ;
14       $\mathcal{L}_{seg}^{real, i} \leftarrow A_s(s^i, S(x^i))$ ;
15    end
16    Update  $D$  by descending its gradient:
17       $\nabla_{\theta_D} \frac{1}{m} \sum_i \mathcal{L}_{adv}^i + \lambda_{cls} \mathcal{L}_{cls}^{real, i}$ ;
18    Update  $S$  by descending its gradient:
19       $\nabla_{\theta_S} \frac{1}{m} \sum_i \mathcal{L}_{seg}^{real, i}$ ;
20  end
21  for  $i = 1, \dots, m$  do
22     $\tilde{x}^i \leftarrow G(z^i, c^i, s_t^i)$ ;
23     $\mathcal{L}_{adv}^i \leftarrow D_d(\tilde{x}^i)$ ;
24     $\mathcal{L}_{cls}^{fake, i} \leftarrow A_c(c^i, D_c(\tilde{x}^i))$ ;
25     $\mathcal{L}_{seg}^{fake, i} \leftarrow A_s(s_t^i, S(\tilde{x}^i))$ ;
26  end
27  Update  $G$  by descending its gradient:
28     $\nabla_{\theta_G} \frac{1}{m} \sum_i -\mathcal{L}_{adv}^i + \lambda_{cls} \mathcal{L}_{cls}^{fake, i} + \lambda_{seg} \mathcal{L}_{seg}^{fake, i}$ ;
29 end
Output: Converged generator parameter  $\theta_G$ .
```

where (x, c) is a pair of real image with its attribute label, $A_c(\cdot, \cdot)$ computes a multi-attribute binary cross-entropy loss by $A_c(a, b) = -\sum_k a_k \log(b_k)$ with a, b being two vectors of identical size $(1 \times n_c)$. Accordingly, we have the classification loss for fake samples by

$$\mathcal{L}_{cls}^{fake} = \mathbb{E}_{z, c, s} [A_c(c, D_c(G(z, c, s)))], \quad (12)$$

which takes the fake image $G(z, c, s)$ as input and guides G to generate attribute-specific images according to the classification information learned from real samples.

4.3 Training Algorithm

Let θ_G, θ_D and θ_S be the parameters of networks G, D and S , respectively. Our objective is to find a converged θ_G with minimized \mathcal{L}_G . When training the proposed SCGAN, a batch of latent vectors are sampled from

a Gaussian distribution $\mathcal{N}(0, 1)$ ¹ denoted as $\{z^i\}_{i=1}^m$, where m is the batch size. A batch of x with its ground-truth s and c are randomly sampled from the joint distribution $\mathbb{P}_{data}(x, c, s)$ of the target dataset, denoted as $\{x^i, c^i, s^i\}_{i=1}^m$. To avoid over-fitting, $\{s^i\}_{i=1}^m$ is randomly shuffled to obtain a batch of target segmentations $\{s_t^i\}_{i=1}^m$ to be input to G . First, we feed D with $\{x^i\}_{i=1}^m$ and $\{c^i\}_{i=1}^m$ and obtain the outputs $\{D_d(x^i)\}_{i=1}^m$ and $\{D_c(x^i)\}_{i=1}^m$. D can be optimized by descending its gradient on \mathcal{L}_D . Then, we train S with $\{x^i\}_{i=1}^m$ and $\{s^i\}_{i=1}^m$ by optimizing the objective \mathcal{L}_{seg}^{real} . D and S are trained repeatedly for five times before training G . G takes $\{z^i\}_{i=1}^m, \{c^i\}_{i=1}^m$ and $\{s_t^i\}_{i=1}^m$ as inputs and generate a batch of fake image $\{G(z^i, c^i, s_t^i)\}_{i=1}^m$, which is input to D and S to calculate the loss terms \mathcal{L}_{adv} , \mathcal{L}_{cls}^{fake} and \mathcal{L}_{seg}^{fake} . Eventually, G is optimized by minimizing the full objective \mathcal{L}_G . (See details in Algorithm 1.)

5 Experiment

In this section, we verify the effectiveness of SCGAN on two datasets with both semantic segmentation and attribute label. We show both visual and quantitative results compared with four representative methods, present the spatial interpolation ability of our model in terms of face synthesis, explore configurations of the generator network to solve a foreground-background mismatch problem, and showcase the model stability and convergence via an ablation study.

5.1 Datasets

Two datasets with semantic segmentation and attribute-level label, *CelebA* (Liu et al., 2015) and *DeepFashion* (Liu et al., 2016; Zhu et al., 2017b) are employed to evaluate the performance of different algorithms.

Large-scale CelebFaces Attributes (*CelebA*) dataset contains 202,599 face images of celebrities with 40 binary attribute labels and 5-point facial landmarks. We use the aligned version and select 5 attributes including black hair, blond hair, brown hair, gender and age in our experiment. This dataset doesn't provide any ground-truth semantic segmentation for the face images. To obtain the semantic segmentation, we apply Dlib (King, 2009) landmarks detector to extract 68-point facial landmarks from the faces images, which separate facial attributes into six different regions. By filling those regions with corresponding semantic index pixel-wisely, semantic segmentation are created.

¹ $\mathcal{N}(0, 1)$ refers to a normal distribution with mean 0 and variation 1. $\mathcal{U}(0, 1)$ refers to a uniform distribution between 0 and 1.

Large-scale Fashion (*DeepFashion*) is a large-scale clothing database, which contains over 800,000 diverse fashion images ranging from well-posed shop images to unconstrained photos from cosumers. In our experiment, we use one of the subsets particularly designed for fashion synthesis task, which selects 78,979 clothing images from the In-shop Clothes Benchmark associated with their attribute labels, captions and semantic segmentations. We use the 18-class color attributes and the provided semantic segmentation in our experiment.

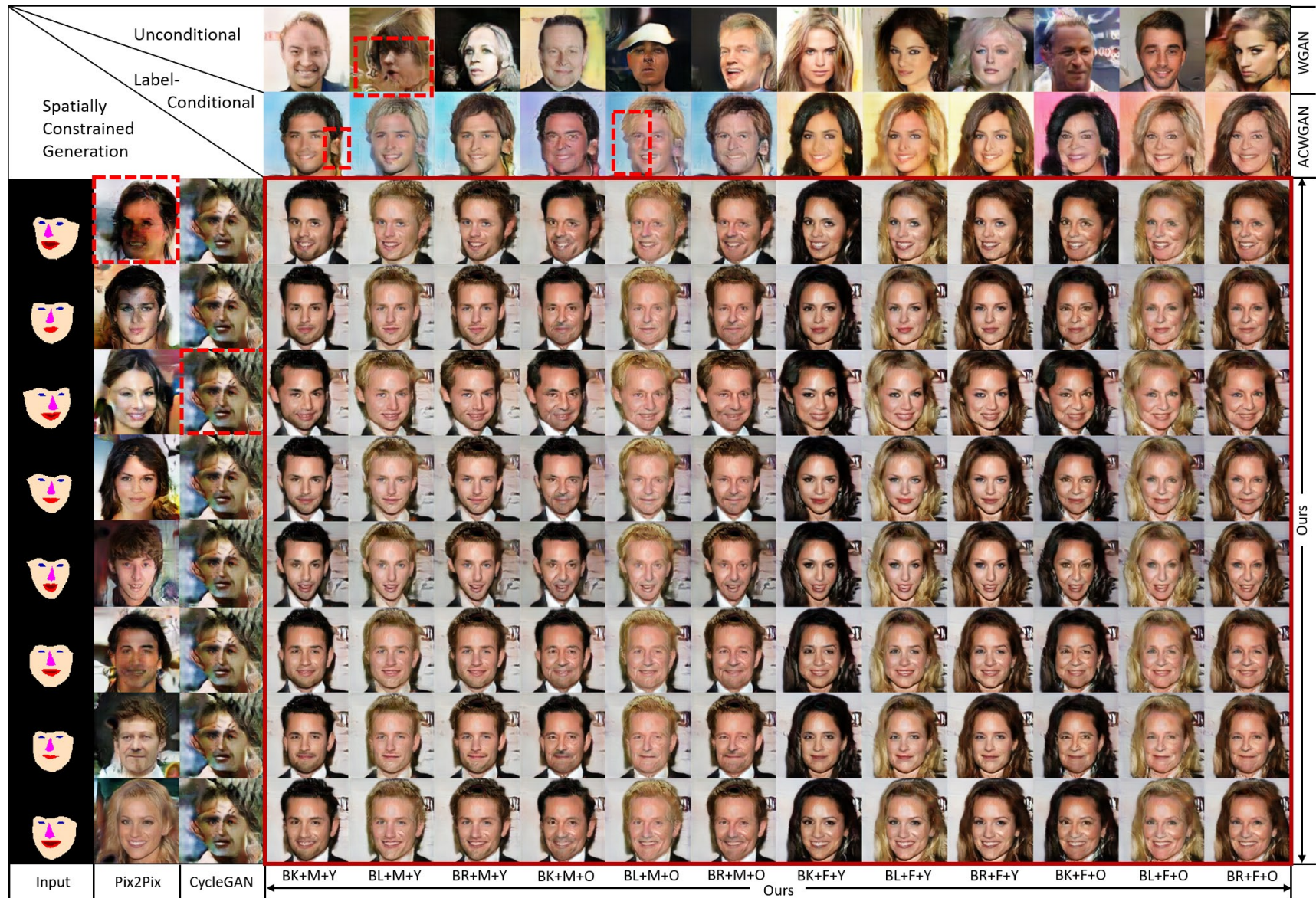


Fig. 4 Comparison with generative models (WGAN, ACWGAN) and image-to-image translation models (Pix2Pix, CycleGAN) on *CelebA* dataset. Our results are shown in the solid red rectangle. Failure cases of the compared methods are highlighted by the dashed red rectangle. (Abbrev.: BK=Black Hair, BL=Blond Hair, BR=Brown Hair, M=Male, F=Female, Y=Young, O=Old.)

5.2 Implementation Details

The network architecture of our proposed SCGAN is shown in the Appendix Table 2. In our generator network, we leverage residual upsampling blocks named as RESBLKUP (as mentioned in Section 4.2.1) instead of transposed convolution layers for upsampling operation. An encoder-decoder structure is used in the segmentor network with several residual blocks (He et al., 2016) names RESBLK as the bottleneck blocks. Detailed architecture of RESBLK and RESBLKUP are shown in Figure 3. Batch normalization layers (Ioffe and Szegedy, 2015) in both the generator and the segmentor networks are replaced with instance normalization layers (Ulyanov et al., 2016). We use leaky ReLU with leakiness 0.2 as the activation function. We follow the PatchGAN structure (Isola et al., 2017) with no normalization method in constructing our discriminator network. Three Adam optimizers (Kingma and Ba, 2014) with β_1 of 0.5 and β_2 of 0.999 are used to optimize our networks. The learning rates are set to 0.0001. The proposed SCGAN is implemented in Pytorch (Paszke et al., 2017). The dimension of input latent vector n_z is 512. The real and generated images of size $(3 \times 128 \times 128)$ are normalized to $[-1, 1]$ as the input images for the discriminator and segmentor.

5.3 Compared Methods

Since the proposed SCGAN takes both conditional attribute labels and semantic segmentation as inputs, we compare our results with two groups of methods, which are the generative models and the image-to-image translation methods.

Improved WGAN (Gulrajani et al., 2017) (abbreviated to WGAN in this section) and ACGAN (Odena et al., 2017) are two representative unconditional and conditional GAN models. However, the network architecture and adversarial loss function of ACGAN is in old fashion, which limits the quality of generated images. Therefore, for a fair comparison, we adopt the training algorithm and network architecture from WGAN into ACGAN to improve the visual quality and stabilize the training process. This method is later referred as ACWGAN in our experiment.

Pix2Pix (Isola et al., 2017) and CycleGAN (Zhu et al., 2017a) are two popular image-to-image translation method, which can take semantic segmentation as input and synthesize realistic images. Pix2Pix requires paired images while CycleGAN is trained in an unpaired way. In our experiment, we use the official implementation released by the authors, train their model, and try our best to tune the parameters to deliver good

results. We are aware that there exists several high-resolution image-to-image translation methods such as Pix2PixHD (Wang et al., 2018b) and PGGAN (Karras et al., 2018). They mention that training high-resolution methods are very time-consuming. Since our target datasets are not high-resolution, synthesizing high-resolution images are beyond the scope of this paper.

5.4 Spatially Constrained Face Synthesis

We first provide comparison results on *CelebA*. The faces generated by different algorithms are shown in Figure 4, which can be divided into three categories, unconditional, label-conditional and spatially constrained generation. The topmost row in Figure 4 gives the unconditional random image generated by WGAN without any controllability on the generating results. The visual quality of WGAN is satisfactory in most cases, however, unfortunately “ghost faces” still occur, as highlighted by the red dashed rectangle. Those “ghost faces” have uncontrolled boundaries of facial attributes. With semantic segmentation as spatial constraints to guide the image generation process, our method could avoid generating such “ghost faces” and always produce reliable and high-quality results. The second row shows the attribute-conditional results generated by ACWGAN with a fixed latent vector z . Compared with their results, our method can still produce much higher visual quality. For ACWGAN results, attribute labels also affect the background color that female images look much warmer than male images. In our results, however, spatial and attribute information is decoupled well from the other unregulated contents determined by input latent vector. With a fixed latent vector, our method can always produce consistent images with a fixed background. Facial attributes can be regulated by input label with no other unrelated contents changed. Due to the high frequency signal from boundaries of attributes in semantic segmentation, our SCGAN could produce a large amount of sharp details which make the results more realistic compared to all the other methods.

Compared to the generative models, our method has additional controllability on spatial domain regulated by input semantic segmentation. We could specify spatial configuration by inputting our target semantic segmentations to the generator. Our method is also superior in general visual quality, especially on the boundaries, since semantic segmentations provide high-frequency signals to the model as additional guidance.

In the spatially constrained generation, the input segmentations are shown in the leftmost column of Figure 4, and the results of Pix2Pix and CycleGAN are shown in the next two columns. The faces generated

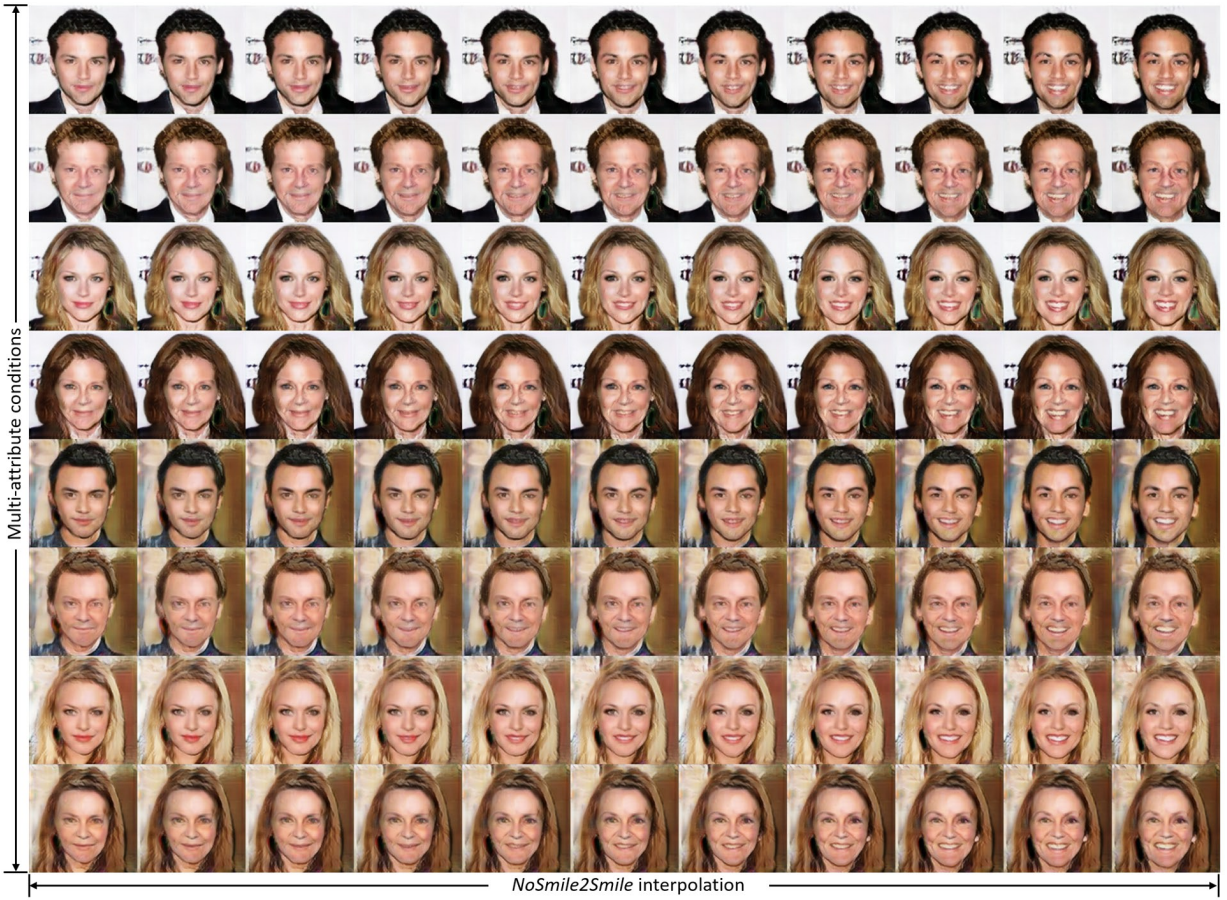


Fig. 5 *NoSmile2Smile* facial expression interpolations. Each row shows a group of interpolated results between a not smiling face and a smiling face with a specific attribute label and a fixed latent vector.

by Pix2Pix are in low quality. CycleGAN even suffers a mode collapse issue that their model only gives a single output no matter the input segmentation. One possible reason is that translating facial segmentation to realistic face is essentially an one-to-many translation. Essentially, those two image-to-image translation methods both assume an one-to-one mapping between input and target domains. Especially for CycleGAN, their cycle-consistency loss which seeks to maintain the contents during a cycle translating forward and backward tends to enforce the one-to-one mapping. However, in this case, when a face image is translated into its semantic segmentation, it is barely possible to translate it back to the original face due to the information lost in the many-to-one translation. Their methods struggle in looking for an one-to-one mapping from the one-to-many mapping and eventually fail to achieve it.

Compared with these image-to-image translation methods, it is worth noting that our method can generate images with variations on facial attributes and other details with a single input. Our model can do one-to-many generations directed by the input latent vector and at-

tribute label, while their methods only provide one-to-one generation. We show that inputting randomly sampled latent vectors can result into diverse images with different background and details in segmentation-to-image synthesis. In summary, our proposed SCGAN enjoys the superiority in terms of diverse variations, controllability and realistic high-quality results over the image-to-image translation methods.

5.5 Interpolation Abilities

Beyond face synthesis, our proposed SCGAN is able to control the orientation and facial expressions of the synthesized faces by feeding corresponding semantic segmentations as guidance. In order to synthesize faces of every intermediate states between two facial orientation and expressions, semantic segmentations of those intermediate states are required as inputs. However, there is a big challenge in obtaining such intermediate semantic segmentations. Since semantic segmentations are represented by a pixel-wise k -channel image, numeric interpolations between two segmentations only result in a



Fig. 6 Two-dimension interpolation results in latent space and between *Left2Right* faces. Each column presents the results of interpolated latent vectors, and each row shows the interpolation results on facial orientations from left face to right face.

fade-in and fade-out effect, which is clearly not a spatial interpolation between two states.

We solve this challenge by interpolating in facial landmarks domain instead of segmentations domain. x - y coordinates of facial landmarks represent their physical locations. Therefore, numeric interpolation between two facial landmarks creates every intermediate states of facial landmarks in spatial domain. We could then construct semantic segmentations from those landmarks to obtain spatial-varying semantic segmentation. By feeding those segmentations with other inputs of latent vector and attribute label fixed, we can generate every intermediate image between face orientations and ex-

pressions. As shown in Figure 5 and 6, SCGAN could generate spatially interpolated faces from left-side face to right-side face (*Left2Right*) and not smiling face to smiling face (*NoSmile2Smile*). It is worth noticing that *Left2Right* interpolation is not just creating mirrored faces. Instead, all the components including the asymmetric hair style “rotate” with the orientation of the head. The *Left2Right* and *NoSmile2Smile* interpolation provides very natural, consistent and realistic results, which encourages many exciting applications such as synthesizing face videos with liveness. All the other generative methods cannot achieve such controllability or deliver the similar spatially interpolated results.



Fig. 7 Comparison with generative models (WGAN, ACWGAN) and image-to-image translation models (Pix2Pix, CycleGAN) on *DeepFashion* dataset. Their failure cases are highlighted in the dashed red rectangle, while the dashed blue rectangle highlights the representative diverse results generated by our proposed SCGAN.

5.6 Spatially Constrained Fashion Synthesis

Comparison results on the *DeepFashion* dataset presented in Figure 7 also demonstrate the advantages of our proposed SCGAN over the other methods. Similar to Figure 4, the input segmentation, results of Pix2Pix and results of CycleGAN are shown in the left three columns. Fashion images generated by WGAN and ACWGAN are shown in the top two rows. The images in the large solid red rectangle are our results from SCGAN with both semantic segmentation and attribute labels and latent vector as inputs. This figure can also be separated into two task, which are segmentation-to-fashion synthesis and latent-vector-to-fashion synthesis. In the task of segmentation-to-fashion synthesis, different from the results on *CelebA* dataset, image-to-image translation methods are capable of producing acceptable results on the *DeepFashion* dataset. This is because that the intrinsic one-to-many property in the *DeepFashion* dataset is not as strong as in the *CelebA* dataset. In the *DeepFashion* dataset, the ability of shape preserving becomes more important than general visual discrimination. However, their results still lack of attribute-level controllability and variations on fashion detail as our results, which are highlighted by the dashed blue rectangle. Our proposed SCGAN can generate fashion images controlled by the input color labels and semantic segmentation, while the input latent vectors encode variant fashion style (e.g. cardigans, T-shirts), diverse pants and shoes, and different color shades and saturation (e.g. dark blue, light blue).

In latent-vector-to-fashion synthesis task, although WGAN can generally produce acceptable results with a large variation and ACWGAN could produce diverse images based on input color labels (red, blue, white and pink), many “ghost images” highlighted by the dashed red rectangle still happen. Unlike face synthesis, fashion synthesis has a large diversity in the shapes of clothes and human bodies. Lacking spatial regulation, WGAN and ACWGAN both produce images with unexpected boundaries which make the generated results seem unrealistic. With our introduced semantic segmentation as the spatial constraints, our proposed SCGAN could produce sharper and more realistic fashion style images with both spatial controllability and attribute-level controllability. As shown in Figure 7, all the components in *DeepFashion* datasets are decoupled into three categories that the whole fashion style is controllable by the input semantic segmentation, color of clothes is controlled by the input attribute label, while the other finer details of fashion design, color shade, even skin color and hair color are determined by the input latent vector.



Fig. 8 Comparison of two training algorithms: (a) Train all networks in SCGAN together. (b) Pretrain segmentor first, then fix its parameters during training the rest of SCGAN.

Table 1 Accuracy of spatial consistency.

Datasets	<i>CelebA</i>	<i>DeepFashion</i>
Shuffled (floor)	0.9204	0.8027
CycleGAN	0.9292	0.8221
Pix2Pix	0.9805	0.8291
SCGAN (ours)	0.9895	0.8323
Original (ceiling)	0.9928	0.8341

5.7 Train the Segmentor Separately

As mentioned in Section 4.2.3 and Algorithm 1, in this paper, we propose the segmentor network to be trained together with the generator and the discriminator networks. Theoretically, our segmentor network can also be trained separately from the other networks using the real images with their ground-truth semantic segmentations. After finishing training the segmentor network, when training the generator and discriminator networks, we can fix the parameters of the pretrained segmentor network to speed up the model convergence and save the memory usage of GPUs. In order to explore the difference in performance between training the segmentor network together and training it separately, we conduct an experiment to compare the visual quality of these two training algorithms. The results are provided in Figure 8.

As a result, we find that pretraining and fixing the segmentor will result in slightly lower visual quality compared with our original algorithm of training all together, especially in the face region. Results in 8(a) seem to have more realistic faces and boundaries compared to results in 8(b). Based on our observation, the interactions between the segmentor, generator and discriminator during their training process lead to a little better visual quality. In conclusion, training the segmentor separately is still a viable and efficient way if saving the memory usage or speeding up the convergence is necessary. Otherwise, the segmentor can be trained together with the rest networks in SCGAN to obtain better visual quality.

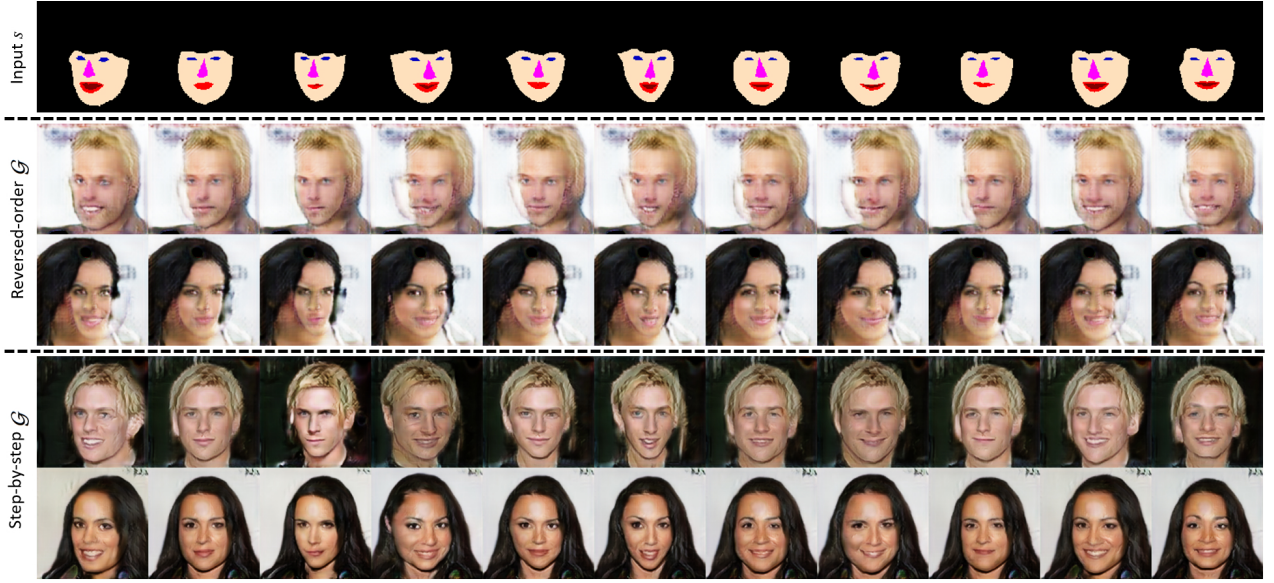


Fig. 9 Explore the generator configuration. This figure shows the input segmentations, the results generated by reversed-order generator, and by the step-by-step generator proposed in SCGAN.

5.8 Quantitative Evaluation

To quantitatively evaluate the effectiveness of spatially constrained image generation, inspired by the evaluation method used in attribute-level conditional image synthesis, we conduct an experiment to examine the spatial consistency between the input semantic segmentation and the generated images from the generator. In this experiment, we use the pretrained segmentor network to estimate the probability of each pixel from the generated images belong to the segmentation classes. Using a maximum operator, we can then obtain an estimated semantic segmentation from the probability matrix. The estimated semantic segmentations are then compared with the original input segmentations to calculate the average accuracy of each input image, which is so called accuracy of spatial consistency.

Unlike ordinary accuracy, this accuracy of spatial consistency has its ceiling value and floor value. The ceiling of this accuracy is calculated by taking real images from the datasets as input to the segmentor network, and comparing the estimated semantic segmentation with their ground-truth values. The floor of this accuracy is calculated by using randomly shuffled unpaired image and segmentation. Since existing GAN based methods cannot achieve spatially constrained generation, we compare our results with the image-to-image translation methods of CycleGAN and Pix2Pix. As shown in Table 1, our SCGAN achieves the best accuracy in both *CelebA* and *DeepFashion* datasets. Our performance is closed to the ceiling accuracy of original datasets, which validates that our method is capable

of generating spatially controllable images that comply accurately with the input semantic segmentations.

5.9 Step-by-Step Generator Configuration

As described in Section 4.2.1, the generator of our proposed SCGAN takes three inputs, a semantic segmentation, a latent vector and an attribute label step by step in orders. One critical issue is that the contents in the synthesized image should be decoupled well to be controlled by those inputs. Otherwise, those inputs may conflict with each other and fail to generate the desired results. To demonstrate that, we reverse the input orders and build a variation of our generator, which takes the latent vector as input for transposed convolution first, then take inputs the semantic segmentation and attribute label. We refer this variant of generator network as the reversed-order G .

As shown in Figure 9, severe foreground-background mismatches happen in the results of reversed-order G that the facial components regulated by the input segmentation cannot be merged correctly with the skin color or hair style determined by the latent vector. To tackle this challenge, we particularly design the generator in a step-by-step way to extract spatial information from semantic segmentation first to construct the basic spatial structure of the synthesized image. It takes the latent vector to add variations to the other unregulated components, and eventually uses attribute label to render attribute-specific contents. As a result, our proposed generator could successfully decouple the contents of synthesized image into controllable inputs.

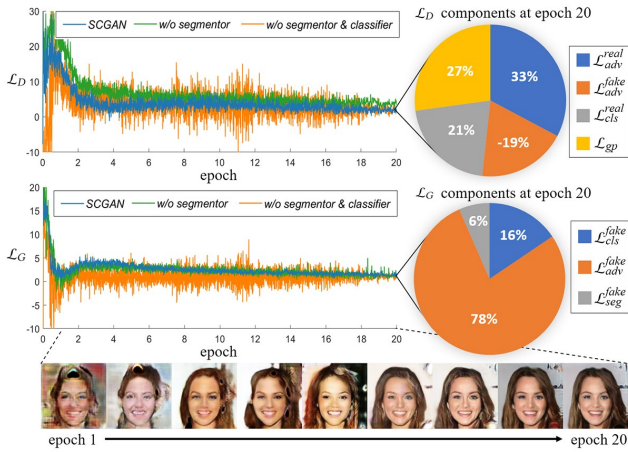


Fig. 10 An ablation study on model convergence contains the plots losses during training and the intermediate generated samples. (better be viewed in color)

This approach solves the foreground-background merging problem and generates spatially controllable and attribute-specific images with variations on other unregulated contents.

5.10 Ablation Study on Model Convergence

Our proposed SCGAN converges fast and stably due to the introduction of the segmentor and the auxiliary classifier. To support this claim, we conduct an ablation study on model convergence by removing segmentor and auxiliary classifier step by step. Figure 10 shows the losses of generator and discriminator during the training process on *CelebA* dataset. The blue plots are the losses of the proposed SCGAN. Green plots are the losses after removing the segmentor network. The orange plots show the losses after removing both the segmentor network and the embedded auxiliary classifier, while all the other things such as model architecture and hyper-parameters kept unchanged.

Observed from this figure, the training process of our SCGAN is much more stable with less vibration on losses. In the plot of discriminator losses, the convergence of SCGAN happens faster and its final loss is smaller than the other two ablation experiments. In the plot of generator losses, even though the proposed SCGAN introduces an additional segmentation loss added to the generator loss, our final losses eventually reach the same level, which means that generator in the proposed SCGAN converges faster. The pie charts show the percentage of each loss components after their convergence at epoch 20, which demonstrates that the segmentation loss and classification loss both play critical roles and cannot be neglected. The bottom part of Figure 10 shows the intermediate generated samples with

the same inputs by SCGAN during its training process. The visual quality of these intermediate generated samples improves gradually as the model converges.

6 Conclusions

In this paper, we proposed SCGAN to introduce spatial constraints in conditional image generation task. We obtained promising visual and quantitative results compared with other popular generative models and image-to-image translation methods on *CelebA* and *DeepFashion* datasets. These results demonstrated that the proposed SCGAN was capable of controlling spatial contents, specifying attributes and improving general visual quality. We particularly designed the generator to take semantic segmentations, latent vectors and attribute labels step by step. We showed that this configuration enabled the ability of interpolating on different dimensions while keep the other contents unchanged. Different configurations of the generator were compared to show that our proposed generator configuration solved the foreground-background mismatch problem. With an ablation study, we validated that the proposed SCGAN was easy and fast to train as the introduced segmentor network accelerated and stabilized the model convergence. Furthermore, we proposed an effective way to obtain accurate and reliable semantic segmentations of all intermediate states for *CelebA* using facial landmarks, which enabled many interesting applications such as the *Left2Right* and *NoSmile2Smile* interpolation. In summary, our method is a useful and effective variant of the GAN, which could be easily adapted to recent high-resolution GAN based image generation models. We hope this work would benefit the target-oriented image synthesis and facilitate the future study on GAN based generative models.

References

- Arjovsky M, Chintala S, Bottou L (2017) Wasserstein generative adversarial networks. In: International Conference on Machine Learning (ICML), pp 214–223
- Berthelot D, Schumm T, Metz L (2017) Began: Boundary equilibrium generative adversarial networks. arXiv preprint arXiv:1703.10717
- Blanz V, Vetter T (1999) A morphable model for the synthesis of 3d faces. In: Proceedings of the 26th annual conference on Computer graphics and interactive techniques, ACM Press/Addison-Wesley Publishing Co., pp 187–194

- Bora A, Price E, Dimakis AG (2018) Ambientgan: Generative models from lossy measurements. In: International Conference on Learning Representations (ICLR)
- Bousmalis K, Silberman N, Dohan D, Erhan D, Krishnan D (2017) Unsupervised pixel-level domain adaptation with generative adversarial networks. In: Proceedings of the The IEEE Conference on Computer Vision and Pattern Recognition (CVPR), IEEE, vol 1, p 7
- Chen X, Duan Y, Houthoofd R, Schulman J, Sutskever I, Abbeel P (2016) Infogan: Interpretable representation learning by information maximizing generative adversarial nets. In: Advances in neural information processing systems (NIPS), pp 2172–2180
- Choi Y, Choi M, Kim M, Ha JW, Kim S, Choo J (2018) Stargan: Unified generative adversarial networks for multi-domain image-to-image translation. In: Proceedings of the IEEE Conference on Computer Vision and Pattern Recognition (CVPR), IEEE
- Chongxuan L, Xu T, Zhu J, Zhang B (2017) Triple generative adversarial nets. In: Advances in Neural Information Processing Systems (NIPS), pp 4088–4098
- Egger B, Schönborn S, Schneider A, Kortylewski A, Morel-Forster A, Blumer C, Vetter T (2018) Occlusion-aware 3d morphable models and an illumination prior for face image analysis. International Journal of Computer Vision pp 1–19
- Genova K, Cole F, Maschinot A, Sarna A, Vlasic D, Freeman WT (2018) Unsupervised training for 3d morphable model regression. In: In Proceedings of the IEEE Conference on Computer Vision and Pattern Recognition (CVPR), IEEE, pp 8377–8386
- Goodfellow I, Pouget-Abadie J, Mirza M, Xu B, Warde-Farley D, Ozair S, Courville A, Bengio Y (2014) Generative adversarial nets. In: Advances in neural information processing systems (NIPS), pp 2672–2680
- Gulrajani I, Ahmed F, Arjovsky M, Dumoulin V, Courville AC (2017) Improved training of wasserstein gans. In: Advances in Neural Information Processing Systems (NIPS), pp 5767–5777
- He K, Zhang X, Ren S, Sun J (2016) Deep residual learning for image recognition. In: In Proceedings of the IEEE Conference on Computer Vision and Pattern Recognition, IEEE, pp 770–778
- Hoffman J, Wang D, Yu F, Darrell T (2016) Fcns in the wild: Pixel-level adversarial and constraint-based adaptation. arXiv preprint arXiv:161202649
- Ioffe S, Szegedy C (2015) Batch normalization: Accelerating deep network training by reducing internal covariate shift. In: International Conference on Machine Learning (ICML), pp 448–456
- Isola P, Zhu JY, Zhou T, Efros AA (2017) Image-to-image translation with conditional adversarial networks. In: Proceedings of the IEEE Conference on Computer Vision and Pattern Recognition (CVPR), IEEE, pp 5967–5976
- Karras T, Aila T, Laine S, Lehtinen J (2018) Progressive growing of GANs for improved quality, stability, and variation. In: International Conference on Learning Representations (ICLR)
- Kim T, Cha M, Kim H, Lee JK, Kim J (2017) Learning to discover cross-domain relations with generative adversarial networks. In: International Conference on Machine Learning (ICML), pp 1857–1865
- King DE (2009) Dlib-ml: A machine learning toolkit. Journal of Machine Learning Research pp 1755–1758
- Kingma DP, Ba J (2014) Adam: A method for stochastic optimization. arXiv preprint arXiv:1412.6980
- Kocaoglu M, Snyder C, Dimakis AG, Vishwanath S (2018) CausalGAN: Learning causal implicit generative models with adversarial training. In: International Conference on Learning Representations (ICLR)
- Krizhevsky A, Hinton G (2009) Learning multiple layers of features from tiny images. Tech. rep.
- LeCun Y, Bottou L, Bengio Y, Haffner P (1998) Gradient-based learning applied to document recognition. Proceedings of the IEEE 86(11):2278–2324
- Ledig C, Theis L, Huszár F, Caballero J, Cunningham A, Acosta A, Aitken AP, Tejani A, Totz J, Wang Z, et al. (2017) Photo-realistic single image super-resolution using a generative adversarial network. In: CVPR, vol 2, p 4
- Li J, Liang X, Wei Y, Xu T, Feng J, Yan S (2017a) Perceptual generative adversarial networks for small object detection. In: Proceedings of the IEEE Conference on Computer Vision and Pattern Recognition (CVPR), IEEE, pp 1951–1959
- Li X, Zhang Y, Zhang J, Chen Y, Li H, Marsic I, Burd RS (2017b) Region-based activity recognition using conditional gan. In: In Proceedings of the ACM on Multimedia Conference (ACMMM), ACM, pp 1059–1067
- Liu MY, Tuzel O (2016) Coupled generative adversarial networks. In: Advances in neural information processing systems (NIPS), pp 469–477
- Liu MY, Breuel T, Kautz J (2017a) Unsupervised image-to-image translation networks. In: Advances in Neural Information Processing Systems (NIPS), pp 700–708
- Liu S, Sun Y, Zhu D, Bao R, Wang W, Shu X, Yan S (2017b) Face aging with contextual generative adversarial nets. In: In Proceedings of the ACM on Multimedia Conference (ACMMM), ACM, pp 82–90

- Liu W, Liu X, Ma H, Cheng P (2017c) Beyond human-level license plate super-resolution with progressive vehicle search and domain priori gan. In: In Proceedings of the ACM on Multimedia Conference (ACMMM), ACM, pp 1618–1626
- Liu Z, Luo P, Wang X, Tang X (2015) Deep learning face attributes in the wild. In: Proceedings of the IEEE International Conference on Computer Vision (ICCV), IEEE, pp 3730–3738
- Liu Z, Luo P, Qiu S, Wang X, Tang X (2016) Deepfashion: Powering robust clothes recognition and retrieval with rich annotations. In: Proceedings of the IEEE Conference on Computer Vision and Pattern Recognition (CVPR, IEEE, pp 1096–1104
- Luc P, Couprie C, Chintala S, Verbeek J (2016) Semantic segmentation using adversarial networks. In: Advances in neural information processing systems (NIPS) Workshop on Adversarial Training
- Mathieu M, Couprie C, LeCun Y (2015) Deep multi-scale video prediction beyond mean square error. arXiv preprint arXiv:151105440
- Matthews I, Xiao J, Baker S (2007) 2d vs. 3d deformable face models: Representational power, construction, and real-time fitting. *International journal of computer vision* 75(1):93–113
- Mirza M, Osindero S (2014) Conditional generative adversarial nets. arXiv preprint arXiv:14111784
- Miyato T, Kataoka T, Koyama M, Yoshida Y (2018) Spectral normalization for generative adversarial networks. In: International Conference on Learning Representations (ICLR)
- Odena A, Olah C, Shlens J (2017) Conditional image synthesis with auxiliary classifier gans. In: International Conference on Machine Learning (ICML), pp 2642–2651
- Paszke A, Gross S, Chintala S, Chanan G, Yang E, DeVito Z, Lin Z, Desmaison A, Antiga L, Lerer A (2017) Automatic differentiation in pytorch
- Radford A, Metz L, Chintala S (2015) Unsupervised representation learning with deep convolutional generative adversarial networks. arXiv preprint arXiv:151106434
- Susskind J, Anderson A, Hinton GE (2010) The toronto face dataset. Technical Report UTML TR 1:2010
- Ulyanov D, Vedaldi A, Lempitsky VS (2016) Instance normalization: The missing ingredient for fast stylization. arXiv preprint arXiv:160708022
- Vetter T (1998) Synthesis of novel views from a single face image. *International journal of computer vision* 28(2):103–116
- Wang TC, Liu MY, Zhu JY, Liu G, Tao A, Kautz J, Catanzaro B (2018a) Video-to-video synthesis. In: Advances in Neural Information Processing Systems (NIPS)
- Wang TC, Liu MY, Zhu JY, Tao A, Kautz J, Catanzaro B (2018b) High-resolution image synthesis and semantic manipulation with conditional gans. In: Proceedings of the IEEE Conference on Computer Vision and Pattern Recognition (CVPR), IEEE, vol 1, p 5
- Yi Z, Zhang HR, Tan P, Gong M (2017) Dualgan: Unsupervised dual learning for image-to-image translation. In: Proceedings of the IEEE International Conference on Computer Vision, IEEE, pp 2868–2876
- Yu L, Zhang W, Wang J, Yu Y (2017) Seqgan: Sequence generative adversarial nets with policy gradient. In: AAAI Conference on Artificial Intelligence (AAAI), pp 2852–2858
- Zhang H, Xu T, Li H, Zhang S, Wang X, Huang X, Metaxas D (2017) Stackgan++: Realistic image synthesis with stacked generative adversarial networks. arXiv preprint arXiv:171010916
- Zhang Y, Gan Z, Carin L (2016) Generating text via adversarial training. In: Advances in Neural Information Processing Systems (NIPS) workshop on Adversarial Training
- Zhao Y, Deng B, Huang J, Lu H, Hua XS (2017) Stylized adversarial autoencoder for image generation. In: In Proceedings of the ACM on Multimedia Conference (ACMMM), ACM, pp 244–251
- Zhu JY, Park T, Isola P, Efros AA (2017a) Unpaired image-to-image translation using cycle-consistent adversarial networks. In: Proceedings of the IEEE International Conference on Computer Vision, IEEE
- Zhu S, Fidler S, Urtasun R, Lin D, Loy CC (2017b) Be your own prada: Fashion synthesis with structural coherence. In: Proceedings of the IEEE International Conference on Computer Vision (ICCV), IEEE, pp 1689–1697

Appendix: Networks Architecture

The detailed architecture of the generator, discriminator and segmentor networks in the proposed SCGAN are provided in Table 2. The shape of the intermediate result after each layer is also displayed in the right column. In summary, the generator takes a semantic segmentation, a latent vector and an attribute label as inputs step by step to synthesize a target image as described in Section 4.2.1. The discriminator network has a discrimination output and a classification output which share the same weights except the last layer. The segmentor network adopts an encoder-decoder architecture with a few residual blocks as the bottle neck layers.

Table 2 Network architecture of SCGAN. (Abbrev: L=Layer; CONV=Convolutional layer; FC=Fully connected layer; RES-BLK=Residual block; RESBLKUP=Residual block with upsampling; DECONV=Transposed convolutional layer; N=Number of neurons; K=Kernel Size; S=Stride; P=Padding; CONCAT=Concatenate; IN=Instance Normalization; RELU=Rectified Linear Unit; IRELU=leaky RELU; n_z =Dimension of latent vector; n_c =Number of attributes; n_s =Number of segmentation classes)

L	Generator	Output Shape
a	<i>Semantic segmentation</i>	$n_s \times 128 \times 128$
1	CONV-(N64,K4,S2,P1),IN,RELU	$64 \times 64 \times 64$
2	CONV-(N128,K4,S2,P1),IN,RELU	$128 \times 32 \times 32$
3	CONV-(N256,K4,S2,P1),IN,RELU	$256 \times 16 \times 16$
4	CONV-(N512,K4,S2,P1),IN,RELU	$512 \times 8 \times 8$
b	<i>Latent vector</i>	$n_z \times 1 \times 1$
b1	FC-(N8192),IN,RELU	$64 \times 8 \times 8$
5	CONCAT 4 with b1	$576 \times 8 \times 8$
6	RESBLKUP-(N64),IN,RELU	$512 \times 16 \times 16$
7	RESBLKUP-(N64),IN,RELU	$256 \times 32 \times 32$
c	<i>Attribute label</i>	$n_c \times 1 \times 1$
c1	EXPAND	$n_c \times 32 \times 32$
8	CONCAT 7 with c1	$256+n_c \times 32 \times 32$
9	RESBLKUP-(N64),IN,RELU	$128 \times 64 \times 64$
10	RESBLKUP-(N64),IN,RELU	$64 \times 128 \times 128$
11	CONV-(N3,K3,S1,P1),TANH	$3 \times 128 \times 128$
L	Discriminator	Output Shape
a	<i>Input image</i>	$3 \times 128 \times 128$
1	CONV-(N64,K4,S2,P1),IRELU	$64 \times 64 \times 64$
2	CONV-(N128,K4,S2,P1),IRELU	$128 \times 32 \times 32$
3	CONV-(N256,K4,S2,P1),IRELU	$256 \times 16 \times 16$
4	CONV-(N512,K4,S2,P1),IRELU	$512 \times 8 \times 8$
5	CONV-(N1024,K4,S2,P1),IRELU	$1024 \times 4 \times 4$
6	CONV-(N2048,K4,S2,P1),IRELU	$2048 \times 2 \times 2$
b	CONV-(N1,K3,S1,P1)	$1 \times 2 \times 2$
c	CONV-(Nn_c ,K3,S1,P1)	$n_c \times 1 \times 1$
L	Segmentor	Output Shape
a	<i>Input image</i>	$3 \times 128 \times 128$
1	CONV-(N64,K4,S2,P1),IN,RELU	$64 \times 64 \times 64$
2	CONV-(N128,K4,S2,P1),IN,RELU	$128 \times 32 \times 32$
3	RESBLK-(N128,K3,S1,P1),IN,RELU	$128 \times 32 \times 32$
4	RESBLK-(N128,K3,S1,P1),IN,RELU	$128 \times 32 \times 32$
5	RESBLK-(N128,K3,S1,P1),IN,RELU	$128 \times 32 \times 32$
6	RESBLK-(N128,K3,S1,P1),IN,RELU	$128 \times 32 \times 32$
7	DECONV-(N64,K4,S2,P1),IN,RELU	$64 \times 64 \times 64$
8	DECONV-(N32,K4,S2,P1),IN,RELU	$32 \times 128 \times 128$
9	CONV-(Nn_s ,K3,S1,P1)	$n_s \times 128 \times 128$